Photochemical & Photobiological Sciences

Accepted Manuscript

This is an *Accepted Manuscript*, which has been through the Royal Society of Chemistry peer review process and has been accepted for publication.

Accepted Manuscripts are published online shortly after acceptance, before technical editing, formatting and proof reading. Using this free service, authors can make their results available to the community, in citable form, before we publish the edited article. We will replace this *Accepted Manuscript* with the edited and formatted *Advance Article* as soon as it is available.

You can find more information about *Accepted Manuscripts* in the Information for Authors.

Please note that technical editing may introduce minor changes to the text and/or graphics, which may alter content. The journal's standard Terms & Conditions and the Ethical guidelines still apply. In no event shall the Royal Society of Chemistry be held responsible for any errors or omissions in this *Accepted Manuscript* or any consequences arising from the use of any information it contains.

ROYAL SOCIETY OF CHEMISTRY

www.rsc.org/pps

New cyanopyridone based luminescent liquid crystalline materials: Synthesis and characterization

Ahipa T.N., and Airody Vasudeva Adhikari *

Department of Chemistry, National Institute of Technology Karnataka, Surathkal, Mangalore - 575025, India.

* Corresponding author. Tel.: +91 8242474046; fax: +918242474033.

E-mail addresses: avachem@gmail.com, avadhikari123@yahoo.co.in, avchem@nitk.ac.in.

Abstract: A new series of 4-(3,4-bis(akyloxy)phenyl)-6-(4-((1-(4-cyano- or 4-nitro- benzyl)-1*H*-1,2,3-triazol-4-yl)methoxy)phenyl)-2-oxo-1,2-dihydropyridine-3-carbonitriles carrying terminal di-alkoxy chain lengths (*viz*. octyloxy, decyloxy, dodecyloxy, tetradecyloxy and hexadodecyloxy) as well as terminal polar groups –CN or $–NO_2$ have been designed and synthesized successfully as luminescent mesogens. Their thermotropic behaviors have been studied by means of differential scanning calorimetry and polarized optical microscopy. The supramolecular organizations in them have been explored by temperature dependent X-ray diffraction method and their photophysical properties have been investigated using UV-visible and fluorescence spectral methods. The mesogenic study reveals that the presence of hydrogen bond as well as dimerization between the molecules is mainly responsible for the formation of ambient temperature hexagonal columnar phase (Col_h) in the new molecules. Their photophysical study indicates that the compounds exhibit a strong absorption band at ~ 370 nm and a blue emission band at ~ 466 nm with good quantum yields of ~ 0.62 when compared to quinine sulphate (Φ_f=0.54), in chloroform. Also, the compounds show slightly red shift in absorption band with increased solvent polarity. In liquid crystalline films, they display a bathochromic shift in emission band because of the intimate overlap of molecular cores in the hexagonal columnar phase.

Keywords: Luminescent mesogen; Cyanopyridone, Triazole, Photophysical property.

Introduction

Luminescent mesogens are fascinating materials that constitute a realistic challenge in flat-panel technologies because of their intrinsic luminescent and liquid crystalline properties.[1-9] Their high charge carrier mobilities and ability to develop defect-free layers as well as molecular self-organization contribute effectively for improving the device performance. In this context, prominent efforts have been made by the researchers in the design and development of new luminescent mesogens. Generally, it has been observed that in design of luminescent mesogens, the molecular shape has a dominant role in the formation of liquid crystalline state.[10, 11] Eventually, the design of new luminescent mesogens involves proper selection of core fragment, linking group and terminal functionality. Based on this, various heterocycle centered luminescent mesogens have been designed keeping in view of their ability to impart lateral and/or longitudinal dipoles with respect to the changes in the molecular shape.[12-14] In such molecules, the presence of heteroatoms like S, O and N, being more polarizable than carbon, results in considerable changes in the corresponding liquid crystalline phases and/or physical properties of the observed phases.[15]

Amongst various heterocyclic mesogens, the pyridone based liquid crystalline materials are well established in the literature. Particularly, 2-pyridone derivatives with pyridine as a core were shown to form well-defined hexagonal columnar phase via hydrogen bonded dimer.[16-19] Further, compounds carrying 1,2,3-triazole system were demonstrated to possess good liquid crystalline behavior along with electron transport ability because of the unique properties such as high molecular anisotropy, chemical as well as thermal stability exhibited by 1,2,3-triazole moiety.[20-25]

Keeping this in view, in the present work, we thought of selecting 3-cyanopyridone moiety as a highly polarizable luminescent core and 1,4-disubstituted 1,2,3-triazole as electron deficient entity to build a molecular network that would combine both liquid crystalline property and luminescent behavior with electron transport ability. Accordingly, we designed a new series of luminescent mesogens, *viz*. 4-(3,4-bis(akyloxy)phenyl)-6-(4-((1-(4-cyano- or 4-nitro- benzyl)-1*H*-1,2,3-triazol-4-yl)methoxy)phenyl)-2-oxo-1,2-dihydropyridine-3-carbonitriles (**5a-j**), wherein 3-cyanopyridone acts as a luminescent core, 1,4-disubstituted 1,2,3-triazole behaves as an electron deficient system, -CN or $-NO_2$ acts as polar group and variable alkoxy chain lengths (m=8-16 (only even)) as terminal substituents create additional polarizability and flexibility to the resultant motifs. The newly designed molecules were synthesized from one pot synthesis by reacting acetyl functionalized 1,4-disubstituted 1,2,3-triazole, 3,4-bis(alkyloxy)benzaldehyde, ethyl cyanoacetate and ammonium acetate. They were characterized by FTIR, ^{1}H NMR, ^{13}C NMR, mass spectral and elemental analyses. Their liquid crystalline properties were investigated by subjecting the compounds to polarized optical microscopy (POM), differential scanning calorimetry (DSC) and powder X-ray diffraction (PXRD) analyses. Their photophysical properties were determined using UV-visible and fluorescence studies. Finally, crystal structure study on intermediate compound **3a** was carried out using single crystal X-ray diffraction (SCXRD) analysis.

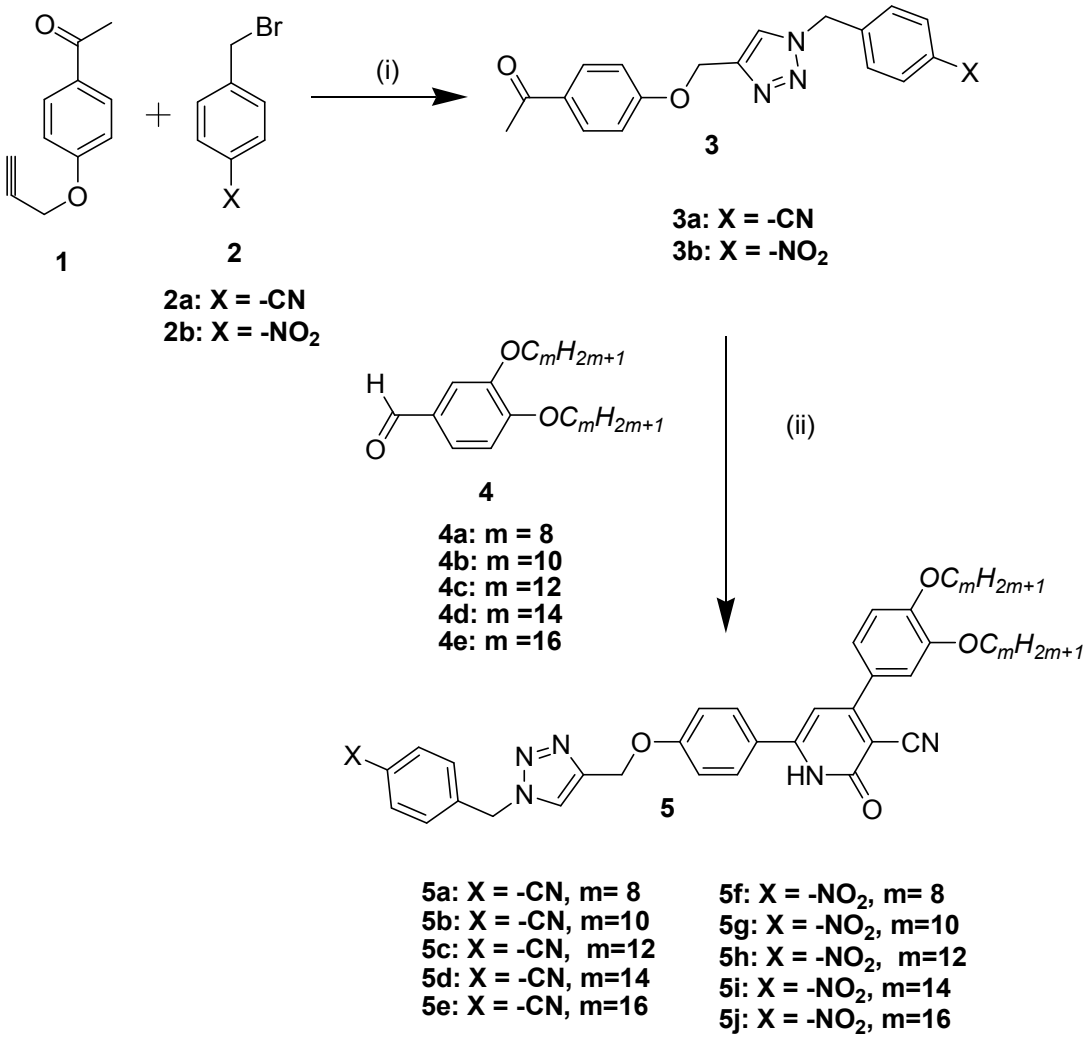

Scheme 1 Synthetic route for the synthesis of target compounds **5a-j**. Reagents and conditions: (i) NaN_3, CuI (10 mol%), ethanol-water, 80 °C, 12h; (ii) ethyl cyanoacetate, ammonium acetate, 1,4-dioxane, reflux, 12h.

Experimental section

Materials and methods

The organic reagents and solvents were obtained from commercial sources. The organic reagents were used without further purification. But, the organic solvents were used after drying them by traditional methods. The target and intermediate compounds were purified by recrystallization from analytical grade solvents. The purity of sample was confirmed by thin

layer chromatography (Merck 60 Kieselgel F 254) and elemental analyses (Flash EA1112 analyzer). The UV-visible and fluorescence spectra were taken in GBC Cintra 101 and Perkin Elmer LS55 fluorescence spectrophotometers, respectively. Infrared spectra were recorded on a Nicolet Avatar 5700 FTIR (Thermo Electron Corporation). ^{1}H and ^{13}C NMR spectra were recorded on a Bruker Avance DPX spectrometer at 400 MHz using DMSO-d_6 or $CDCl_3$ as the solvent, with tetramethylsilane as internal standard. Mass spectra (ESI) were recorded on Waters ZQ-4000 liquid chromatography-mass spectrometer. The phase transition temperatures were determined using a SHIMADZU DSC-60 differential scanning calorimeter with a heating rate of 10 $^{\circ}C\ min^{-1}$ (the apparatus was calibrated with indium, 156.6 $^{\circ}C$). About 3 mg of sample was hermetically sealed in an aluminium pan and placed in a nitrogen atmosphere. The sequence of phases and phase transition temperatures were identified by observing the textures and their changes under the polarizing optical microscope (POM). Polarized light microscopic studies were carried out using a Leitz Ortholux II Pol-BK microscope equipped with a Mettler FP82HT hot stage (temperature stabilization within ±0.1 K). Powder X-ray diffraction data were collected using a Philips X-pert diffractometer with *CuKα* radiation (λ = 1.54 Å) over the angular range $2° \leq 2\theta \leq 40°$, with a step width of 0.0167° at room temperature, calibrated against Silicon Powder (NIST-SRM 640c) standards. Le Bail profile analysis in the JANA2000 suite was used to refine the X-ray diffraction data.[26] The background was estimated by the Legendre polynomial function consisting of 15 coefficients, and the peak shapes were described by a pseudo-Voigt function varying five profile coefficients. A scale factor, a zero error factor, and shape were refined. A suitable sized crystals of **3a** was mounted using a Mitigen micromount and single crystal data collection was done on a Bruker Smart X2S bench top diffractometer equipped with a micro-focus MoKα radiation (λ = 0.71073) at room temperature.[27] The machine was operated at 50kV

and 1mA. Data reduction was performed using SAINTPLUS. Scaling, absorption correction was done using SADABS, all embedded in the Apex2 software suite.[27] The crystal structure was solved by direct methods using XS and the structure refinement was done using XL in the SHELXTL package.[28] The position and thermal parameters of all the non-hydrogen atoms were refined. The hydrogens were fixed in geometrically calculated positions and refined isotropically. The ORTEP diagrams and packing diagrams were created using Mercury 3.0.

Synthesis

The synthesis of final compounds **5a-j** involves two important steps as shown in scheme 1: firstly, the one pot synthesis of acetyl functionalized 1,4-disubstituted 1,2,3-triazole unit via slightly modified click reaction; secondly, the single step synthesis of final compounds by reacting acetyl functionalized 1,4-disubstituted 1,2,3-triazole, 3,4-bis(alkyloxy)benzaldehyde, ethyl cyanoacetate and ammonium acetate. The progress of the reaction was monitored by thin layer chromatography and the structures of the new compounds were confirmed by spectral methods. The intermediate compounds **4a-e** were synthesized according to the reported procedure.[29]

For the construction of 1,4-disubstituted 1,2,3-triazoles, generally, copper catalyzed click reaction involving organic azides and alkynes is employed because of its outstanding merits such as high conversion efficiency and no side product formation.[30-32] Therefore, the slightly modified click reaction, reported by our group has been successfully employed for the synthesis of required new 1,2,3-triazole derivatives **3a,b**.[33] Here, one pot synthesis of 1,4-disubstituted 1,2,3-triazoles **3a,b** has been achieved by the three component reaction of organic halides, alkynes and sodium azide in water and ethanol mixture; thereby one can avoid the preparation and isolation

of highly unstable and potentially explosive organic azides. The final compounds carrying cyanopyridones were built by *in situ* condensation followed by cyclization of three components in one pot reaction.

General procedure for the preparation of acetyl functionalized 1,4-disubstituted 1,2,3-triazole ***(3a, b)***

A mixture of 1-(4-(prop-2-ynyloxy)phenyl)ethanone (**1**, 1.0 mmol), 4-(bromomethyl)benzonitrile (**2a,** 1.1 mmol**)** or 1-(bromomethyl)-4-nitrobenzene (**2b,** 1.1 mmol), sodium azide (1.2 mmol) in presence of copper iodide (10 mol%) was heated at 80 °C in ethanol and water (5 ml) mixture for 12 h. After cooling, water was added and stirred for 30 min at room temperature. The obtained solid was filtered off, washed with ethanol and recrystallized from ethanol to get pure product.

4-((4-((4-Acetylphenoxy)methyl)-1H-1,2,3-triazol-1-yl)methyl)benzonitrile ***(3a)***: Yield 69 %, m.p. 126-128 °C. FTIR (cm^{-1}): 2919, 2869, 2232, 1676, 1607, 1359, 1258, 1180, 1050, 812. ^{1}H NMR (400 MHz, $CDCl_3$) δ: 7.92 (d, *J*=8.8 Hz, 2H, Ar-H), 7.80 (s, 1H, Ar-H(Triazole)), 7.66 (d, *J*=8 Hz, 2H, Ar-H), 7.35 (d, *J*=8 Hz, 2H,Ar-H), 7.00 (d, *J*=8.8 Hz, 2H, Ar-H), 5.60 (s, 2H, -OCH_2-), 5.26 (s, 2H, Ar-CH_2-), 2.55 (s, 3H, -COCH_3). ^{13}C NMR (100 MHz, $CDCl_3$) δ (ppm); 196.65, 161.87, 144.38, 139.59, 134.90, 131.65, 130.92, 128.45, 122.90, 118.04, 114.42, 112.95, 77.00, 53.50, 51.91, 26.33. MS (m/z): 333.1 $(M+H)^+$. Anal. Calcd. For. $C_{19}H_{16}N_4O_2$: C. 68.66; H. 4.85; N. 16.86. Found: C. 68.88; H. 4.93; N. 16.91.

1-(4-((1-(4-Nitrobenzyl)-1H-1,2,3-triazol-4-yl)methoxy)phenyl)ethanone ***(3b)***: Yield 76 %, m.p. 131-133 °C. FTIR (cm^{-1}): 2923, 2851, 1664, 1602, 1513, 1421, 1348, 1254, 1172, 1050, 804. ^{1}H NMR (400 MHz, $CDCl_3$) δ: 8.20 (d, *J*=8.8 Hz, 2H, Ar-H), 7.91 (d, *J*=8.8 Hz, 2H, Ar-H), 7.64

(s, 1H, Ar-H(Triazole)), 7.41 (d, *J*=8 Hz, 2H,Ar-H), 7.00 (d, *J*=8.8 Hz, 2H, Ar-H), 5.65 (s, 2H, -OCH_2-), 5.26 (s, 2H, Ar-CH_2-), 2.53 (s, 3H, -$COCH_3$). ^{13}C NMR (100 MHz, $CDCl_3$) δ (ppm); 196.67, 161.86, 144.44, 141.34, 130.92, 128.63, 128.25, 124.33, 122.97, 114.42,114.01, 77.32, 61.99, 53.22, 26.31. MS (m/z): 353.1 $(M+H)^+$. Anal. Calcd. For. $C_{18}H_{16}N_4O_4$: C. 61.36; H. 4.58; N. 15.90. Found: C. 61.63; H. 4.61; N. 15.86.

*General procedure for the synthesis of 4-(3,4-bis(akyloxy)phenyl)-6-(4-((1-(4-cyano- or 4-nitro-benzyl)-1H-1,2,3-triazol-4-yl)methoxy)phenyl)-2-oxo-1,2-dihydropyridine-3-carbonitriles (**5a-j**)*

A mixture of acetyl functionalized 1,4-disubstituted 1,2,3-triazole **3** (1.0 mmol), 3,4-bis(alkyloxy)benzaldehyde **4** (1.0 mmol), ethyl cyanoacetate (1.1 mmol) ammonium acetate (8.0 mmol) in 1,4-dioxane (5 mL) was refluxed for 12 h. The obtained precipitate was filtered off, washed successively with 1,4-dioxane, followed by ethyl acetate and finally recrystallized from ethanol/DMF to afford the pure product **5**.

*4-(3,4-Bis(octyloxy)phenyl)-6-(4-((1-(4-cyanobenzyl)-1H-1,2,3-triazol-4-yl)methoxy)phenyl)-2-oxo-1,2-dihydropyridine-3-carbonitrile (**5a**)*: Yield 72 %. FTIR (cm^{-1}): 2918, 2847, 2217, 1723, 1580, 1508, 1465, 1440, 1264, 1181, 1017, 801. ^{1}H NMR (400 MHz, $CDCl_3$) δ: 8.12 (s, 1H, N-H), 7.92 (d, *J*=8.8 Hz, 2H, Ar-H), 7.80 (s, 1H, Ar-H(Triazole)), 7.73 (s, 1H, Ar-H), 7.66 (d, *J*=8 Hz, 2H, Ar-H), 7.61 (s, 1H, Ar-H(Pyridone)), 7.35 (d, *J*=8 Hz, 2H,Ar-H), 7.12 (d, *J*=8.4 Hz, 2H, Ar-H), 7.00 (d, *J*=8.8 Hz, 2H, Ar-H), 5.60 (s, 2H, -OCH_2-), 5.26 (s, 2H, Ar-CH_2-), 4.04 (t, *J*=6.2 Hz, 4H, -OCH_2-), 1.75-1.24 (m, 24H, -CH_2-), 0.83 (t, *J*=6.6 Hz, 6H, -CH_3). ^{13}C NMR (100 MHz, $CDCl_3$) δ (ppm); 154.88,127.55, 113.94, 77.30, 77.00, 76.68, 69.26, 69.12, 31.91, 29.60, 29.34, 29.05, 28.96, 26.00, 22.68, 14.22, 14.09. MS (m/z): 741.4 $(M+H)^+$. Anal. Calcd. For. $C_{45}H_{52}N_6O_4$: C. 72.95; H. 7.07; N. 11.34. Found: C. 73.19; H. 7.01; N. 11.43.

*4-(3,4-Bis(decyloxy)phenyl)-6-(4-((1-(4-cyanobenzyl)-1H-1,2,3-triazol-4-yl)methoxy)phenyl)-2-oxo-1,2-dihydropyridine-3-carbonitrile (**5b**)*: Yield 77 %. FTIR (cm^{-1}): 2917, 2849, 2217, 1723,

1580, 1508, 1467, 1440, 1264, 1180, 1017, 801. ^{1}H NMR (400 MHz, $CDCl_3$) δ: 8.12 (s, 1H, N-H), 7.92 (d, *J*=8.8 Hz, 2H, Ar-H), 7.80 (s, 1H, Ar-H(Triazole)), 7.73 (s, 1H, Ar-H), 7.66 (d, *J*=8 Hz, 2H, Ar-H), 7.61 (s, 1H, Ar-H(Pyridone)), 7.35 (d, *J*=8 Hz, 2H,Ar-H), 7.12 (d, *J*=8.4 Hz, 2H, Ar-H), 7.00 (d, *J*=8.8 Hz, 2H, Ar-H), 5.60 (s, 2H, -OCH_2-), 5.26 (s, 2H, Ar-CH_2-), 4.04 (t, *J*=6.6 Hz, 4H, -OCH_2-), 1.61-1.23 (m, 32H, -CH_2-), 0.84 (t, *J*=6.6 Hz, 6H, -CH_3). ^{13}C NMR (100 MHz, $CDCl_3$) δ (ppm); 154.85,127.57, 113.94, 77.32, 77.00, 76.68, 69.26, 69.12, 31.91, 29.60, 29.34, 29.05, 28.96, 26.00, 22.68, 14.22, 14.09. MS (m/z): 797.5 $(M+H)^+$. Anal. Calcd. For. $C_{49}H_{60}N_6O_4$: C. 73.84; H. 7.59; N. 10.54. Found: C. 74.12; H. 7.67; N. 10.63.

*4-(3,4-Bis(dodecyloxy)phenyl)-6-(4-((1-(4-cyanobenzyl)-1H-1,2,3-triazol-4-yl)methoxy)phenyl)-2-oxo-1,2-dihydropyridine-3-carbonitrile (**5c**)*: Yield 81 %. FTIR (cm^{-1}): 2919, 2852, 2218, 1723, 1580, 1508, 1467, 1440, 1264, 1180, 1017, 804. ^{1}H NMR (400 MHz, $CDCl_3$) δ: 8.12 (s, 1H, N-H), 7.92 (d, *J*=8.8 Hz, 2H, Ar-H), 7.80 (s, 1H, Ar-H(Triazole)), 7.73 (s, 1H, Ar-H), 7.66 (d, *J*=8 Hz, 2H, Ar-H), 7.61 (s, 1H, Ar-H(Pyridone)), 7.35 (d, *J*=8 Hz, 2H,Ar-H), 7.12 (d, *J*=8.4 Hz, 2H, Ar-H), 7.00 (d, *J*=8.8 Hz, 2H, Ar-H), 5.60 (s, 2H, -OCH_2-), 5.26 (s, 2H, Ar-CH_2-), 4.04 (t, *J*=6.6 Hz, 4H, -OCH_2-), 1.61-1.24 (m, 40H, -CH_2-), 0.84 (s, 6H, -CH_3). ^{13}C NMR (100 MHz, $CDCl_3$) δ (ppm); 154.87, 127.55, 124.34, 113.94, 112.34, 77.31, 77.00, 76.68, 69.26, 69.12, 62.36, 31.93, 29.63,29.60, 29.40, 29.36, 29.06, 28.96, 26.01, 25.94, 22.69, 14.22, 14.10. MS (m/z): 853.5 $(M+H)^+$. Anal. Calcd. For. $C_{53}H_{68}N_6O_4$: C. 74.61; H. 8.03; N. 9.85. Found: C. 74.88; H. 8.10; N. 9.89.

*4-(3,4-Bis(tetradecyloxy)phenyl)-6-(4-((1-(4-cyanobenzyl)-1H-1,2,3-triazol-4-yl)methoxy)phenyl)-2-oxo-1,2-dihydropyridine-3-carbonitrile (**5d**)*: Yield 68 %. FTIR (cm^{-1}): 2919, 2849, 2217, 1725, 1580, 1508, 1467, 1440, 1264, 1182, 1017, 806. ^{1}H NMR (400 MHz, $CDCl_3$) δ: 8.12 (s, 1H, N-H), 7.92 (d, *J*=8.8 Hz, 2H, Ar-H), 7.80 (s, 1H, Ar-H(Triazole)), 7.73

(s, 1H, Ar-H), 7.66 (d, *J*=8 Hz, 2H, Ar-H), 7.61 (s, 1H, Ar-H(Pyridone)), 7.35 (d, *J*=8 Hz, 2H,Ar-H), 7.12 (d, *J*=8.4 Hz, 2H, Ar-H), 7.00 (d, *J*=8.8 Hz, 2H, Ar-H), 5.60 (s, 2H, -OCH_2-), 5.26 (s, 2H, Ar-CH_2-), 4.04 (t, *J*=6.6 Hz, 4H, -OCH_2-), 1.61-1.23 (m, 48H, -CH_2-), 0.84 (t, *J*=6.6 Hz, 6H, -CH_3). ^{13}C NMR (100 MHz, $CDCl_3$) δ (ppm); 154.84, 127.58, 124.37, 113.94, 112.31, 77.32, 77.00, 76.68, 69.26, 69.12, 62.36, 31.93, 29.63,29.60, 29.40, 29.36, 29.06, 28.96, 26.01, 25.94, 22.69, 14.22, 14.10. MS (m/z): 909.6 $(M+H)^+$. Anal. Calcd. For. $C_{57}H_{76}N_6O_4$: C. 75.29; H. 8.42; N. 9.24. Found: C. 75.59; H. 8.49; N. 9.30.

*4-(3,4-Bis(hexadecyloxy)phenyl)-6-(4-((1-(4-cyanobenzyl)-1H-1,2,3-triazol-4-yl)methoxy)phenyl)-2-oxo-1,2-dihydropyridine-3-carbonitrile (**5e**)*: Yield 83 %. FTIR (cm^{-1}): 2917, 2849, 2217, 1723, 1580, 1508, 1469, 1440, 1264, 1180, 1017, 804. ^{1}H NMR (400 MHz, $CDCl_3$) δ: 8.12 (s, 1H, N-H), 7.92 (d, *J*=8.8 Hz, 2H, Ar-H), 7.80 (s, 1H, Ar-H(Triazole)), 7.73 (s, 1H, Ar-H), 7.66 (d, *J*=8 Hz, 2H, Ar-H), 7.61 (s, 1H, Ar-H(Pyridone)), 7.35 (d, *J*=8 Hz, 2H,Ar-H), 7.12 (d, *J*=8.4 Hz, 2H, Ar-H), 7.00 (d, *J*=8.8 Hz, 2H, Ar-H), 5.65 (s, 2H, -OCH_2-), 5.28 (s, 2H, Ar-CH_2-), 4.06 (t, *J*=6.4 Hz, 4H, -OCH_2-), 1.61-1.23 (m, 56H, -CH_2-), 0.84 (t, *J*=6.6 Hz, 6H, -CH_3). ^{13}C NMR (100 MHz, $CDCl_3$) δ (ppm); 154.86, 127.58, 124.33, 113.94, 112.34, 77.32, 77.00, 76.68, 69.26, 69.12, 62.36, 31.93, 29.63,29.60, 29.40, 29.36, 29.06, 28.96, 26.01, 25.94, 22.69, 14.22, 14.10. MS (m/z): 965.6 $(M+H)^+$. Anal. Calcd. For. $C_{61}H_{84}N_6O_4$: C. 75.89; H. 8.77; N. 8.71. Found: C. 76.16; H. 8.88; N. 8.66.

*4-(3,4-Bis(octyloxy)phenyl)-6-(4-((1-(4-nitrobenzyl)-1H-1,2,3-triazol-4-yl)methoxy)phenyl)-2-oxo-1,2-dihydropyridine-3-carbonitrile (**5f**)*: Yield 75 %. FTIR (cm^{-1}): 2919, 2850, 2216, 1723, 1580, 1508, 1440, 1263, 1180, 1018, 801. ^{1}H NMR (400 MHz, $CDCl_3$) δ: 8.23 (d, *J*=8.4 Hz, 2H, Ar-H), 8.12 (s, 1H, N-H), 7.93 (d, *J*=8.8 Hz, 2H, Ar-H), 7.73 (s, 1H, Ar-H(Triazole)), 7.62 (s, 1H, Ar-H), 7.45 (s, 1H, Ar-H(Pyridone)), 7.41 (d, *J*=8.4 Hz, 2H, Ar-H), 7.00 (d, *J*=8.8 Hz,

2H,Ar-H), 6.91 (d, *J*=8.4 Hz, 2H, Ar-H), 5.60 (s, 2H, -OCH_2-), 5.26 (s, 2H, Ar-CH_2-), 4.04 (t, *J*=6.2 Hz, 2H, -OCH_2-), 1.75-1.24 (m, 24H, -CH_2-), 0.83 (t, *J*=6.6 Hz, 6H, -CH_3). ^{13}C NMR (100 MHz, $CDCl_3$) δ (ppm); 163.26, 154.84, 153.98, 149.13, 127.59, 124.32, 116.41, 113.88, 112.31, 77.32, 77.00, 76.68, 69.24, 69.11, 62.35, 31.54, 31.49, 29.69, 29.00, 28.91, 25.66, 25.59, 22.57, 14.21, 13.98. MS (m/z): 761.4 $(M+H)^+$. Anal. Calcd. For. $C_{44}H_{52}N_6O_6$: C. 69.45; H. 6.89; N. 11.04. Found: C. 69.72; H. 6.97; N. 11.13.

*4-(3,4-Bis(decyloxy)phenyl)-6-(4-((1-(4-nitrobenzyl)-1H-1,2,3-triazol-4-yl)methoxy)phenyl)-2-oxo-1,2-dihydropyridine-3-carbonitrile (**5g**)*: Yield 78 %. FTIR (cm^{-1}): 2916, 2852, 2219, 1725, 1580, 1508, 1442, 1263, 1180, 1018, 801. ^{1}H NMR (400 MHz, $CDCl_3$) δ: 8.23 (d, *J*=8.4 Hz, 2H, Ar-H), 8.12 (s, 1H, N-H), 7.93 (d, *J*=8.8 Hz, 2H, Ar-H), 7.73 (s, 1H, Ar-H(Triazole)), 7.62 (s, 1H, Ar-H), 7.45 (s, 1H, Ar-H(Pyridone)), 7.41 (d, *J*=8.4 Hz, 2H, Ar-H), 7.00 (d, *J*=8.8 Hz, 2H,Ar-H), 6.91 (d, *J*=8.4 Hz, 2H, Ar-H), 5.60 (s, 2H, -OCH_2-), 5.26 (s, 2H, Ar-CH_2-), 4.04 (t, *J*=6.2 Hz, 2H, -OCH_2-), 1.61-1.23 (m, 32H, -CH_2-), 0.84 (t, *J*=6.6 Hz, 6H, -CH_3). ^{13}C NMR (100 MHz, $CDCl_3$) δ (ppm); 163.28, 154.84, 153.96, 149.13, 127.54, 116.41, 113.88, 112.31, 77.32, 77.00, 76.68, 69.24, 69.11, 62.35, 31.54, 31.49, 29.69, 29.00, 28.91, 25.66, 25.59, 22.57, 14.21, 13.98. MS (m/z): 817.5 $(M+H)^+$. Anal. Calcd. For. $C_{48}H_{60}N_6O_6$: C. 70.56; H. 7.40; N. 10.29. Found: C. 70.79; H. 7.47; N. 10.23.

*4-(3,4-Bis(dodecyloxy)phenyl)-6-(4-((1-(4-nitrobenzyl)-1H-1,2,3-triazol-4-yl)methoxy)phenyl)-2-oxo-1,2-dihydropyridine-3-carbonitrile (**5h**):* Yield 64 %. FTIR (cm^{-1}): 2913, 2851, 2218, 1723, 1580, 1509, 1440, 1263, 1182, 1018, 801. ^{1}H NMR (400 MHz, $CDCl_3$) δ: 8.23 (d, *J*=8.4 Hz, 2H, Ar-H), 8.12 (s, 1H, N-H), 7.93 (d, *J*=8.8 Hz, 2H, Ar-H), 7.73 (s, 1H, Ar-H(Triazole)), 7.62 (s, 1H, Ar-H), 7.45 (s, 1H, Ar-H(Pyridone)), 7.41 (d, *J*=8.4 Hz, 2H, Ar-H), 7.00 (d, *J*=8.8 Hz, 2H,Ar-H), 6.91 (d, *J*=8.4 Hz, 2H, Ar-H), 5.60 (s, 2H, -OCH_2-), 5.26 (s, 2H, Ar-CH_2-), 4.04 (t,

J=6.2 Hz, 2H, -OC<u>H</u>$_2$-), 1.61-1.24 (m, 40H, -C<u>H</u>$_2$-), 0.84 (s, 6H, -C<u>H</u>$_3$). ^{13}C NMR (100 MHz, $CDCl_3$) δ (ppm); 163.24, 154.84, 153.94, 149.13, 127.55, 124.32, 116.41, 113.88, 112.34, 77.32, 77.00, 76.68, 69.24, 62.35, 31.54, 29.69, 29.00, 28.91, 25.66, 25.59, 22.57, 14.21, 13.98. MS (m/z): 873.5 $(M+H)^+$. Anal. Calcd. For. $C_{52}H_{68}N_6O_6$: C. 71.53; H. 7.85; N. 9.63. Found: C. 71.82; H. 7.79; N. 9.70.

*4-(3,4-Bis(tetradecyloxy)phenyl)-6-(4-((1-(4-nitrobenzyl)-1H-1,2,3-triazol-4-yl)methoxy)phenyl)-2-oxo-1,2-dihydropyridine-3-carbonitrile (**5i**)*: Yield 73 %. FTIR (cm^{-1}): 2914, 2850, 2218, 1723, 1580, 1508, 1440, 1265, 1180, 1019, 806. ^{1}H NMR (400 MHz, $CDCl_3$) δ: 8.23 (d, *J*=8.4 Hz, 2H, Ar-<u>H</u>), 8.12 (s, 1H, N-<u>H</u>), 7.93 (d, *J*=8.8 Hz, 2H, Ar-<u>H</u>), 7.73 (s, 1H, Ar-<u>H</u>(Triazole)), 7.62 (s, 1H, Ar-H), 7.45 (s, 1H, Ar-<u>H</u>(Pyridone)), 7.41 (d, *J*=8.4 Hz, 2H, Ar-<u>H</u>), 7.00 (d, *J*=8.8 Hz, 2H,Ar-<u>H</u>), 6.91 (d, *J*=8.4 Hz, 2H, Ar-<u>H</u>), 5.60 (s, 2H, -OCH_2-), 5.26 (s, 2H, Ar-C<u>H</u>$_2$-), 4.04 (t, *J*=6.2 Hz, 2H, -OC<u>H</u>$_2$-), 1.61-1.23 (m, 48H, -C<u>H</u>$_2$-), 0.84 (t, *J*=6.6 Hz, 6H, -C<u>H</u>$_3$). ^{13}C NMR (100 MHz, $CDCl_3$) δ (ppm); 163.27, 154.84, 153.94, 149.13, 127.56, 124.32, 116.41, 113.88, 112.31, 77.32, 76.68, 69.11, 62.35, 31.54, 31.49, 29.00, 28.91, 25.66, 25.59, 22.57, 14.21, 13.98. MS (m/z): 929.6 $(M+H)^+$. Anal. Calcd. For. $C_{56}H_{76}N_6O_6$: C. 72.38; H. 8.24; N. 9.04. Found: C. 72.68; H. 8.29; N. 9.12.

*4-(3,4-Bis(hexadecyloxy)phenyl)-6-(4-((1-(4-nitrobenzyl)-1H-1,2,3-triazol-4-yl)methoxy)phenyl)-2-oxo-1,2-dihydropyridine-3-carbonitrile (**5j**)*: Yield 67 %. FTIR (cm^{-1}): 2919, 2850, 2218, 1725, 1580, 1508, 1442, 1263, 1180, 1019, 801. ^{1}H NMR (400 MHz, $CDCl_3$) δ: 8.23 (d, *J*=8.4 Hz, 2H, Ar-<u>H</u>), 8.12 (s, 1H, N-<u>H</u>), 7.93 (d, *J*=8.8 Hz, 2H, Ar-<u>H</u>), 7.73 (s, 1H, Ar-<u>H</u>(Triazole)), 7.62 (s, 1H, Ar-H), 7.45 (s, 1H, Ar-<u>H</u>(Pyridone)), 7.41 (d, *J*=8.4 Hz, 2H, Ar-<u>H</u>), 7.00 (d, *J*=8.8 Hz, 2H,Ar-<u>H</u>), 6.91 (d, *J*=8.4 Hz, 2H, Ar-<u>H</u>), 5.60 (s, 2H, -OCH_2-), 5.26 (s, 2H, Ar-C<u>H</u>$_2$-), 4.04 (t, *J*=6.2 Hz, 2H, -OC<u>H</u>$_2$-), 1.61-1.23 (m, 56H, -C<u>H</u>$_2$-), 0.84 (t, *J*=6.6 Hz, 6H, -C<u>H</u>$_3$). ^{13}C NMR (100

MHz, $CDCl_3$) δ (ppm); 163.29, 154.84, 153.93, 149.13, 127.59, 124.32, 116.44, 113.88, 112.31, 77.32, 77.00, 76.68, 69.24, 62.35, 31.54, 31.49, 29.69, 29.00, 28.91, 25.66, 25.59, 22.57, 14.21, 13.98. MS (m/z): 985.6 $(M+H)^+$. Anal. Calcd. For. $C_{60}H_{84}N_6O_6$: C. 73.14; H. 8.59; N. 8.53. Found: C. 73.39; H. 8.66; N. 8.45.

Results and discussion

Synthesis

The synthetic route for the preparation of target compounds **5a-j** is shown in Scheme 1. The intermediate acetyl functionalized 1,4-disubstituted 1,2,3-triazole compound **3** was prepared from one pot reaction between acetophenone derivative **1** and substituted benzyl bromide **2** via slightly modified click reaction in ethanol-water mixture. The another intermediate 3,4-*bis*(alkoxy)benzaldehyde **4** was synthesized by reacting 3,4-dihydroxybenzaldehyde with various alkylbromides using Williamson method. Finally, cyanopyridone derivatives **5a-j** were obtained by one pot reaction of acetyl functionalized 1,2,3-triazole **3**, 3,4-bis(alkoxy)benzaldehyde **4**, ethyl cyanoacetate, and ammonium acetate in 1,4-dioxane. The target compounds were well characterized with spectral methods and their purity was established with elemental analysis.

Crystal structure analysis for compound 3a

Superior quality crystals of **3a** were grown by slow evaporation of chloroform/methanol solutions for the determination of X-ray crystal structure and the crystal data are presented in Table S1 (ESI†). The compound **3a** crystallizes in monoclinic crystal system with *P 21/c* space group and cell parameters are a=20.3809(14) Å, b=5.5940(4) Å, c=15.3584(11) Å, V=1683.91Å^3 with Z=4. The molecular structure of compound **3a** with atom labeling is shown in Figure S1 (ESI†).

The molecular structure of acetyl functionalized 1,2,3-triazole **3a** is found to be non-planar as evidenced by the observed large torsion angles of -91.3(3)° (C9-N3-C8-C1) made by methylbenzonitrile ring with 1,2,3-triazole ring, while a torsion angle of 31.5(3)° (C9-C10-C11-O1) made by 4-((4-acetylphenoxy)methyl ring with 1,2,3-triazole ring. Further, the crystal structure of **3a** involves various kinds of non-conventional hydrogen bonds, *viz.* C-H···N and C-H···O interactions (Figure 1). The two kinds of C-H···N interactions are observed, in which one kind of C-H···N interaction is formed between the H9 atom of 1,2,3-triazole ring and the neighboring molecule carrying N1 atom of 1,2,3-triazole ring with the bond distance of 2.409 Å (C9-H9···N1). Similarly, second kind of C-H···N interaction is formed by nitrogen atom of terminal cyano group and the nearby aromatic protons, with the bond distance of 2.622 Å (N2···H6-C6). In addition to C-H···N interactions, one kind of C-H···O hydrogen bond is identified between the oxygen atom of acetyl group and the nearby aromatic protons, with the bond distance of 2.628 Å (C19-H19···O2). Thus, these interactions are responsible for holding the molecules together, which results in the formation of its crystal assembly.

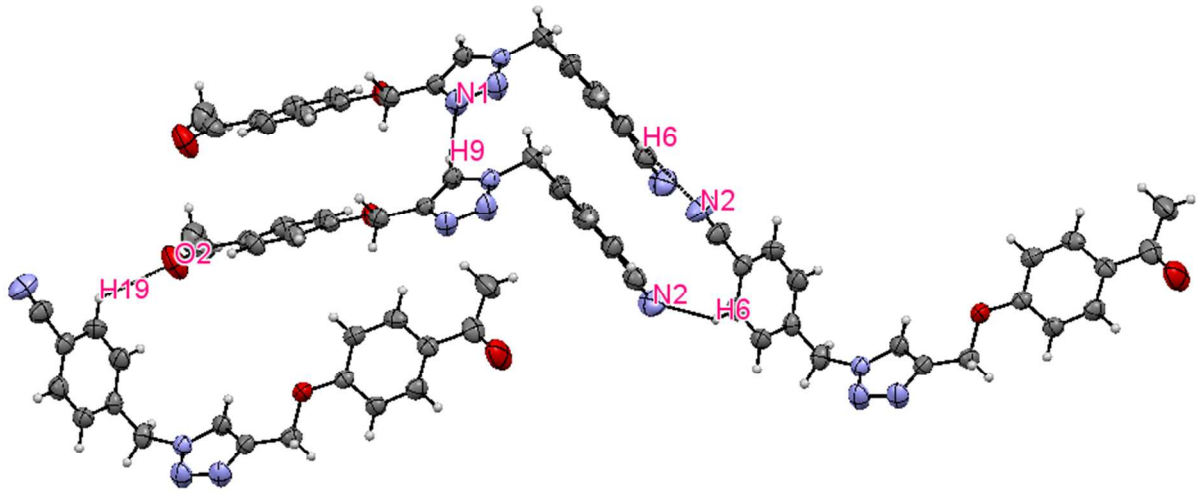

Figure 1 Packing diagram of compound **3a** showing non-conventional hydrogen bonds.

Mesomorphic behavior

The mesophase behavior of **5a-j** was studied by POM and DSC techniques. Their phase transition temperatures and results of enthalpy change are summarized in Table 1. The POM study of compounds **5a-j** confirms the presence of a non-crystalline, soft anisotropic solid at ambient temperature that remains highly viscous until they move into their isotropic liquid state. The well-defined fan-shaped texture characteristic for the hexagonal columnar mesophases (Col_h) are observed both upon heating and cooling processes with the structural variation of terminal alkoxy chain lengths as well as polar substituent's (-CN or $–NO_2$). In addition, DSC thermograms show first-order transitions at the phase transition temperatures. The results are in sound conformity with that of optical observations. The first member of the series, compound **5a** with –CN and two octyloxy chains as terminal substituents is found to exhibit enantiotrophic mesomorphism, wherein, on heating Col_h-I transition is observed at 68.9 $^{\circ}$C, while the phase transition reverts upon cooling. Similar phase transitions are seen in compounds **5b-e** with increase in chain lengths (*i.e.* m=10-16 (even)). But, clearing temperature of compounds has moved from 68.9 $^{\circ}$C (m=8) to 94.1 $^{\circ}$C (m=16) indicating the better Col_h mesophase stability with the increased chain lengths. Also, identical DSC thermograms and mesophase stabilities are perceived in case of compounds **5f-j** with $–NO_2$ as one of the terminal polar substituents. Thereby, it clearly suggests that the variation of chain lengths on the molecular architecture improves the mesophase stability. The fan-shaped columnar texture and DSC trace exhibited by one of the representative compounds **5b** is shown in Figures 2 and 3, respectively.

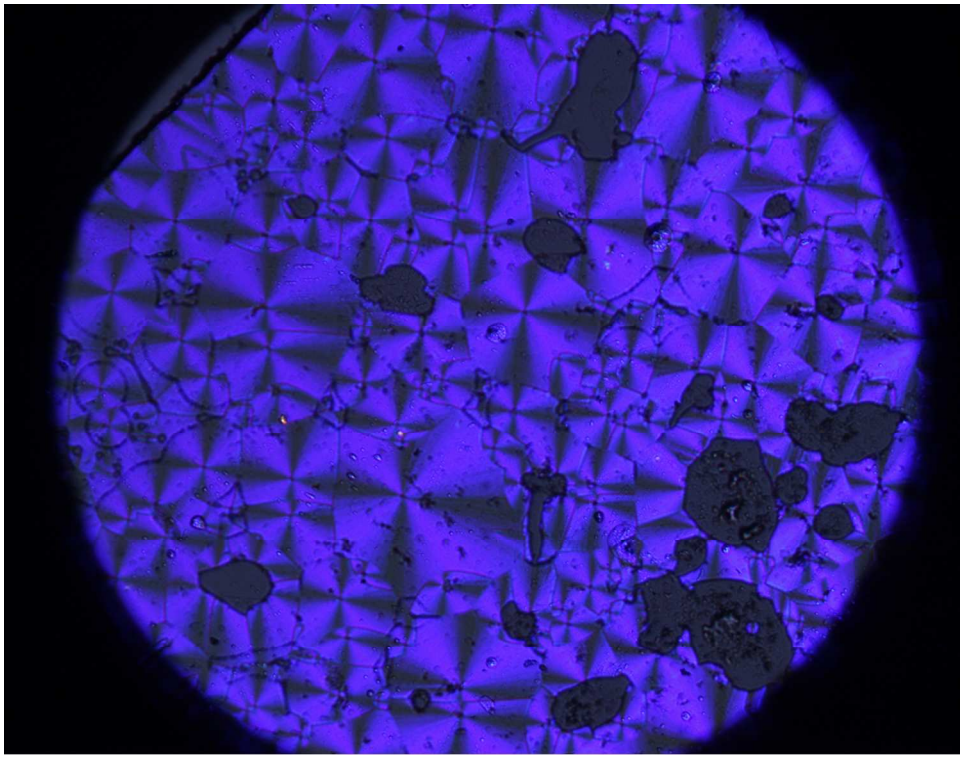

Figure 2 Optical micrograph of **5b** in the Col_h phase at 30 °C

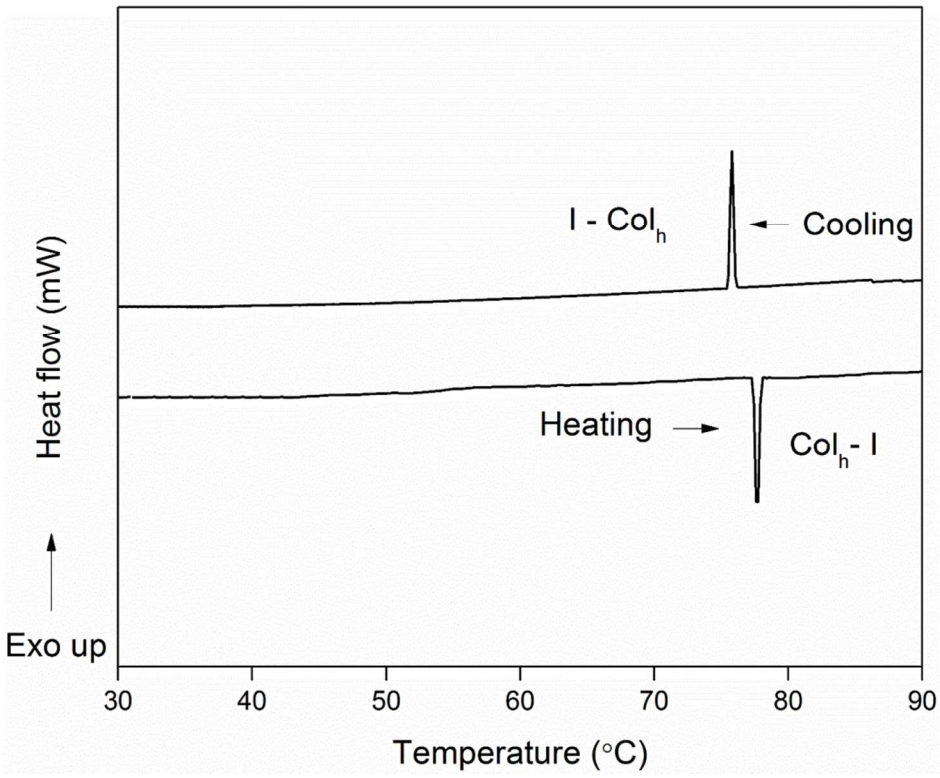

Figure 3 The DSC trace of **5b**

Table 1 Phase transition temperatures and enthalpy changes for **5a-j**

Compound	*m*	X	Transition	Temperature/ °C	ΔH/kJ mol^{-1}
5a	*8*		Col_h-I	68.9	4.5
5b	*10*		Col_h-I	77.7	3.8
5c	*12*	-CN	Col_h-I	80.7	6.1
5d	*14*		Col_h-I	89.8	5.2
5e	*16*		Col_h-I	94.1	6.9
5f	*8*		Col_h-I	61.4	5.4
5g	*10*		Col_h-I	84.1	8.0
5h	*12*	-NO_2	Col_h-I	76.3	6.3
5i	*14*		Col_h-I	82.7	4.0
5j	*16*		Col_h-I	86.9	4.9

Note: Col_h: hexagonal columnar; I: isotropic liquid

In order to investigate the molecular-packing in their liquid crystalline phase, PXRD measurements were performed for the selected mesomorphic compounds **5b** and **5f**. Their results are summarized in Table S2 (ESI†). The powder X-ray diffractogram (Figure 4) obtained for the compound **5b** in liquid crystalline state shows a sharp diffraction peak in the small angle region, which can be indexed to 10 plane of hexagonal lattice of columnar phase. Also, in the wide angle region, appearance of a broad diffused peak centered at 4.11 Å can be attributed to the liquid-like order of the terminal two decyloxy chains. The molecular length of compound **5b** is found to be 27.6 Å as calculated by **MM2** method. The experimentally obtained diameter of the Col_h phase is found to be 48 Å, which is in agreement with the calculated molecular length, only when cyano-terminated compound **5b** is involved in dimer formation, as shown in Figure 4. This kind of dimerization is also observed in the crystal packing of intermediate compound **3a** as depicted in Figure 1. Further, the number of molecules arranged side by side in a single stratum (Z) of

column is calculated to be eight (Z = 8). The observed fact evidences that the construction of eight molecular stratum is mainly because of the dimer formation between the cyano functional groups[34] and the hydrogen bond linking between the cyanopyridone moieties. Also, compound **5f** shows PXRD pattern in its liquid crystalline phase similar to that of compound **5b**. It displays a diffraction peak in the small angle region corresponding to *d*-spacing of 37.96 Å, which is indexed to 10 plane of hexagonal lattice of columnar phase. Further, in the wide angle region, the observed halo peak at 4.31 Å is due to the liquid-like order exerted by the presence of terminal two octyloxy chain lengths in its molecular architecture. Its calculated molecular length, diameter and number of molecules per stratum are found to be 25.38 Å, 44 Å and six, respectively. In this case too, the molecular assembly is predominantly due to the formation of dimer and the presence of hydrogen bond.

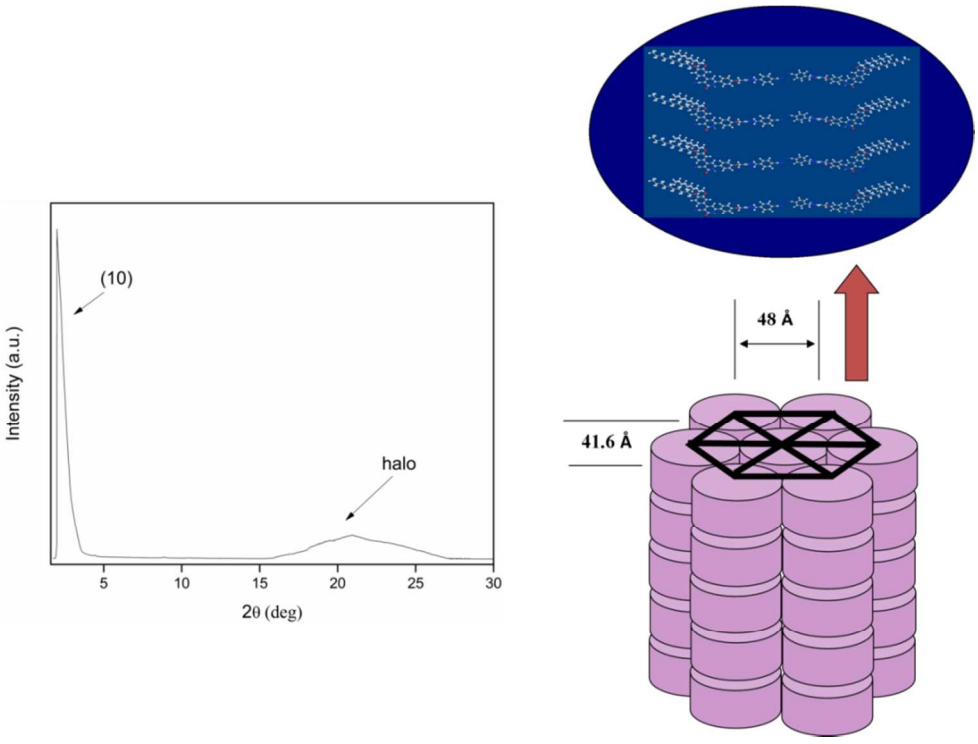

Figure 4 X-ray diffraction pattern and packing model of **5b**

Photophysical properties

The UV-visible absorption spectra of **5a-j** were recorded in chloroform solution at the concentration of 10^{-5} M and the data are summarized in Table 2. The solution absorption spectra of **5a-j** have nearly identical absorption band (λ_{abs}) at ~ 370 nm. Indeed, no considerable change in absorption properties are observed even with the variation of terminal alkoxy chains and the introduction of polar groups such as –CN or $–NO_2$. The observed absorption bands can be attributed to π-π^* transitions in the molecules. The fluorescence spectra were recorded in chloroform solution at the concentration of 10^{-6} M and the emission data are summarized in Table 2. The compounds emit a strong blue fluorescence emission band (λ_{em}) at ~ 466 nm with large Stokes shifts of about 94-99 nm (5529-5733 cm^{-1}). Further, their fluorescence quantum yield (Φ_f) in solution state were determined using the standard procedures, with quinine sulphate in degassed 0.1M sulphuric acid as reference standard (Φ_f = 0.54).[35, 36] Accordingly, the compounds exhibit good quantum yield in the range of 0.60-0.62. In addition, the emission properties of the compounds were investigated in their liquid crystalline state, as they show liquid crystalline phase at room temperature. The liquid crystalline films were prepared over a glass slide by heating the compound to isotropic phase and followed by slow cooling to liquid crystalline phase. These films exhibit strong blue fluorescence emission band in the range of 472-478 nm. Also, in film state, about 10 nm bathochromic shift in the emission band is observed when compared to that of its solution state. The bathochromic shift can be attributed to intimate overlap of molecular cores in the hexagonal columnar phase via. hydrogen bonds that brings the energy levels closer in the film state. Their UV-visible and fluorescence data appear to be identical with respect to their absorption and emission bands, respectively. The UV-visible and fluorescence spectra of **5a** are shown in Figure 5.

Table 2 Optical data of compounds **5a-j**

Compound	λ_{abs} /nm	λ_{em} (solution)/nm	Φ_f (solution)	Stokes shift/nm	λ_{em} (film)/nm
5a	369	468	0.62	99 (5733 cm^{-1})	474
5b	370	466	0.62	96 (5568 cm^{-1})	477
5c	368	462	0.61	94 (5529 cm^{-1})	473
5d	370	466	0.62	96 (5568 cm^{-1})	479
5e	369	468	0.62	99 (5733 cm^{-1})	478
5f	369	467	0.61	98 (5687 cm^{-1})	475
5g	371	465	0.62	94 (5449 cm^{-1})	471
5h	371	468	0.61	97 (5587 cm^{-1})	476
5i	371	466	0.62	95 (5495 cm^{-1})	478
5j	371	468	0.62	97 (5587 cm^{-1})	477

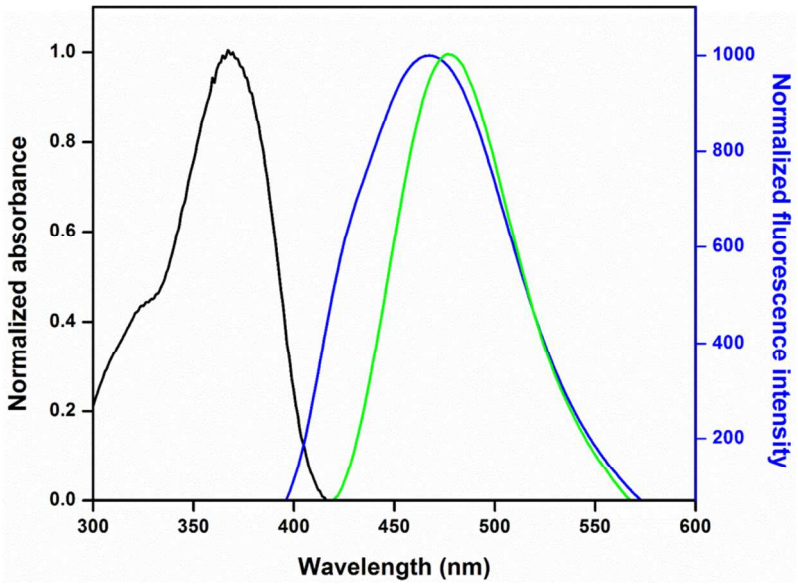

Figure 5 Optical spectra of **5a**, where black line represents UV-visible absorption spectrum in solution state; blue line shows fluorescence emission spectrum in solution state; green line indicates fluorescence spectrum in film state

In order to study the solvatochromic behavior, UV-visible absorption and fluorescence emission spectra of compounds **5b** and **5f** were recorded in various organic solvents (based on polarity) such as hexane, toluene, diethyl ether, chloroform (CF), ethyl acetate (EA), tetrahydrofuran (THF), dichloromethane (DCM), ethanol, methanol, dimethylformamide (DMF), acetonitrile, and dimethyl sulfoxide (DMSO). Their absorption and emission spectra are shown in Figures 6 and 7, respectively. The absorption and emission data measured in various organic solvents are summarized in Table 3. In their absorption spectra, bands are hardly affected by solvent polarity with λ_{abs} (max) being slightly red shifted when the solvent is changed from the hexane (~360 nm) to DMSO (~369 nm). Among the various solvents, the broad spectral bandwidth of 88 nm (as measured by $fwhm_{abs}$) is noticed in DCM solvent for **5b**; similarly, the absorption bandwidth of 82 nm is observed in EA solvent for **5f**. The smaller $fwhm_{abs}$ of **5b** compared to **5f** in EA (72 nm versus 82 nm) suggests a significant difference in equilibrium bond lengths between the ground and excited states in **5f**. However, the fluorescence emission spectra of **5b** and **5f** are not strongly depending on the variation of polar solvents. Among the various solvents, both the compounds display λ_{em} (max) of ~466 nm in CF solvent. Further, the fluorescence quantum yields Φ_f are moderately high (0.20-0.86) in all the solvents used.

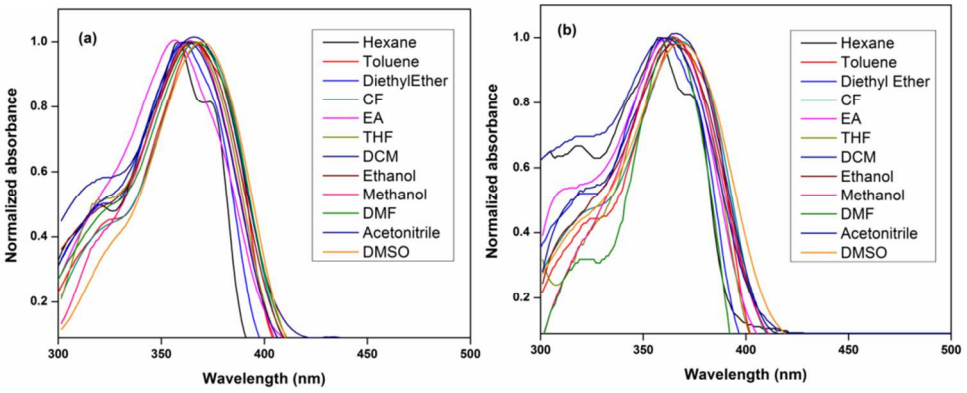

Figure 6 Absorption spectra of compound (a) **5b** and (b) **5f** in various organic solvents

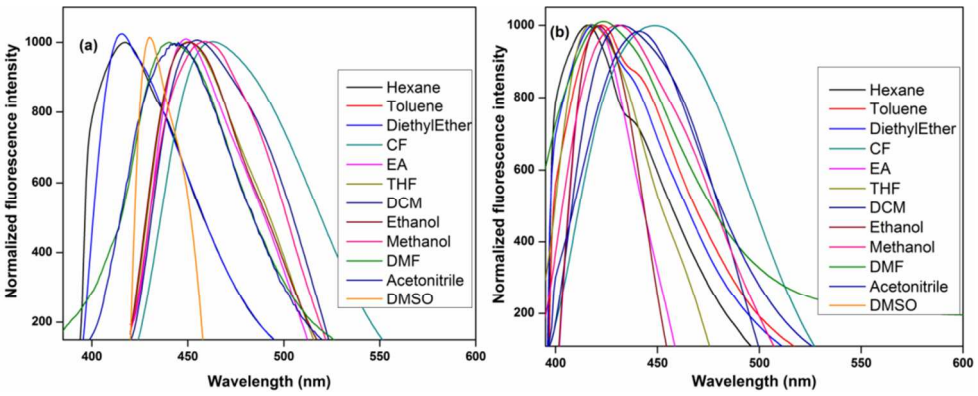

Figure 7 Emission spectra of compound (a) **5b** and (b) **5f** in various organic solvents

Table 3 Optical properties of **5b** and **5f** in various organic solvents along with solvent properties, viz. dielectric constant (**ε**) and refractive index (**η**)

Solvents	ε	η	λ_{abs} (nm)	λ_{em} (nm)	$\Delta\bar{\upsilon}$ (cm^{-1})	$fwhm_{abs}$ (nm)	Φ_f
			Compound 5b				
Hexane	1.88	1.3749	360	416	3739	78	0.68
Toluene	2.38	1.4969	365	415	3300	75	0.83
Diethyl Ether	4.33	1.3524	361	417	3720	60	0.66
CF	4.81	1.4458	370	466	5568	63	0.76
EA	6.02	1.3724	358	452	5809	72	0.48
THF	7.58	1.4072	364	453	5397	76	0.53
DCM	8.93	1.4241	365	458	5563	88	0.61
Ethanol	24.55	1.3614	365	454	5371	67	0.50
Methanol	32.7	1.3284	364	462	5828	61	0.53
DMF	36.71	1.4305	366	444	4800	66	0.81
Acetonitrile	37.50	1.3441	363	445	5076	70	0.65
DMSO	46.68	1.4793	369	433	4006	57	0.24
			Compound 5f				
Hexane	1.88	1.3749	358	415	3837	50	0.78
Toluene	2.38	1.4969	365	422	3701	56	0.82
Diethyl Ether	4.33	1.3524	360	419	3911	57	0.76

CF	4.81	1.4458	369	467	5687	65	0.67
EA	6.02	1.3724	361	420	3891	82	0.20
THF	7.58	1.4072	366	418	3399	59	0.44
DCM	8.93	1.4241	366	432	4174	80	0.60
Ethanol	24.55	1.3614	364	421	3720	74	0.18
Methanol	32.70	1.3284	364	430	4217	64	0.52
DMF	36.71	1.4305	365	433	4303	40	0.86
Acetonitrile	37.50	1.3441	361	442	5076	57	0.65
DMSO	46.68	1.4793	368	420	3364	72	0.54

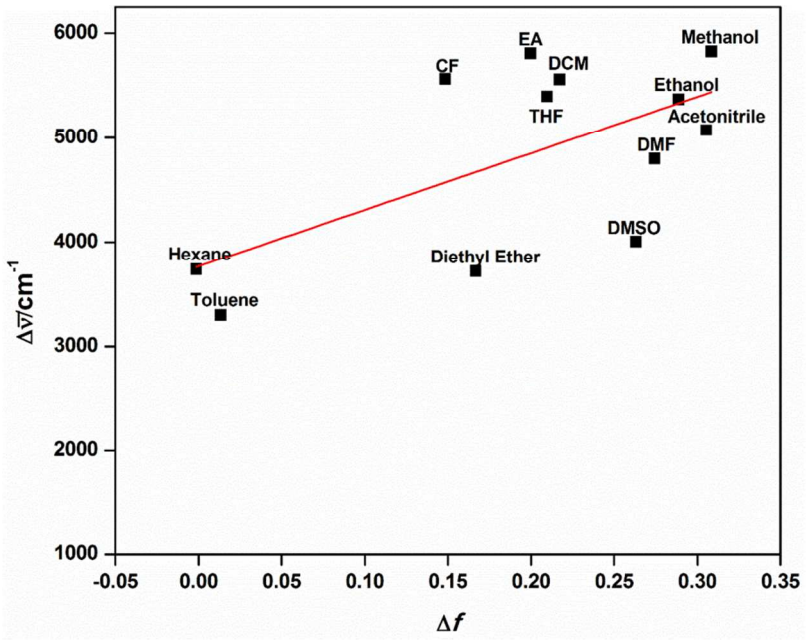

Figure 8 Lippert–Mataga plot for **5b**. The straight line represents the best linear fit to the 12 data points

Generally, solvent induced spectral shifts are interpreted in terms of the Lippert–Mataga[37-39] equation, which describes Stoke shift in terms of the change in the dipole moment of the fluorophore and the dependence of the energy of the dipole on the dielectric constant and refractive index of the solvent. The Lippert–Mataga plot for **5b** and **5f** are shown in Figures 8

and 9, respectively for the 12 solvents listed in Table 3. The observed Lippert−Mataga plot of **5b** shows a poor linear relationship (correlation coefficient $r = 0.6206$) with a slope [5.4 ± 2.0) × 10^3 cm^{-1}] between the Stokes shift $\Delta\bar{\upsilon}$ and solvent orientation polarizibility Δf, while the plot for **5f** exhibits a nonlinear relationship (correlation coefficient $r = 0.1249$) with a slope [8.0 ± 0.9) × 10^2 cm^{-1}]. The observed deviation from linearity has evidenced that the Lippert–Mataga equation considers the general solvent effect and does not reflect the specific solvent–fluorophore interactions, via hydrogen bonding, preferential solvation, acid–base chemistry, or charge-transfer interactions etc.[40-47]

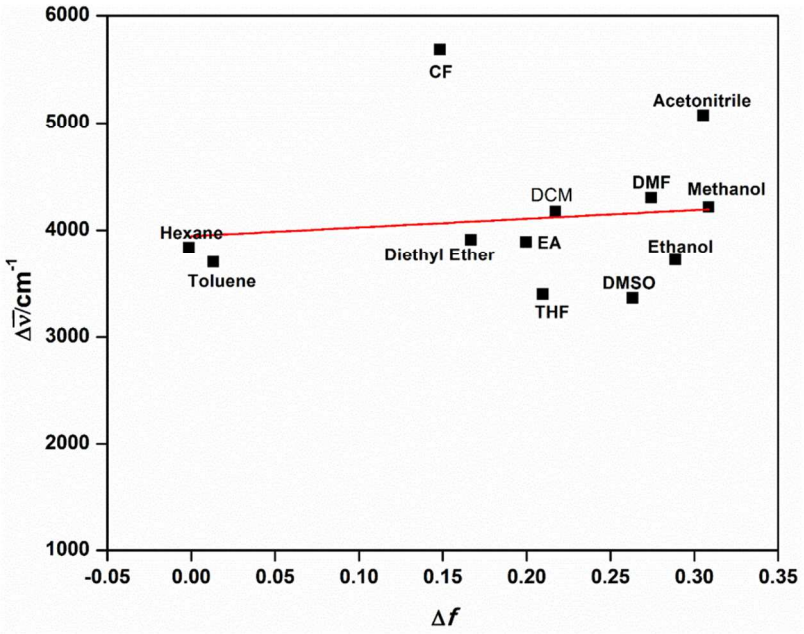

Figure 9 Lippert–Mataga plot for **5f**. The straight line represents the best linear fit to the 12 data points.

In order to account for specific interactions, the most frequently used solvent scales are those of Kamlet and Taft, which can be expressed by the multiple linear equation (1).[48-50]

$$y = y_0 + a_\alpha \alpha + b_\beta \beta + c_{\pi^*} \pi^* \quad (1)$$

In the equation, the parameters α, β and π* represent acidity, basicity and polarity / polarizability, respectively, of a given solvent. The 12 organic solvents and their Kamlet-Taft parameters employed in above equation are tabulated in Table 4. Also, y_0 stands for the physicochemical property of interest in the gas phase; a_α, b_β and c_{π^*} are adjustable coefficients that reflect the sensitivity of the physicochemical property y in a given solvent to the various {α, β and π*} solvent parameters. The physicochemical parameters y analyzed in the present work are the absorption maxima $\bar{\upsilon}_{abs} = 1/\lambda_{abs}(max)$, the emission maxima $\bar{\upsilon}_{em} = 1/\lambda_{em}(max)$, and the Stokes shifts $\Delta\bar{\upsilon} = \bar{\upsilon}_{abs} - \bar{\upsilon}_{em}$ (all in cm^{-1}).

Table 4 Kamlet-Taft (α, β and π^*) and Catalan (SA, SB, SP and SdP) [51] parameters for various organic solvents

Solvent	α	β	π^*	SA	SB	SP	SdP
Hexane	0.00	0.00	-0.04	0.000	0.056	0.616	0.000
Toluene	0.00	0.11	0.54	0.000	0.128	0.782	0.284
Diethyl Ether	0.00	0.47	0.27	0.000	0.562	0.617	0.385
CF	0.20	0.10	0.58	0.047	0.071	0.783	0.614
EA	0.00	0.45	0.55	0.000	0.542	0.656	0.603
THF	0.00	0.55	0.58	0.000	0.591	0.714	0.634
DCM	0.13	0.10	0.82	0.040	0.178	0.761	0.769
Ethanol	0.86	0.75	0.54	0.400	0.658	0.633	0.783
Methanol	0.98	0.66	0.60	0.605	0.545	0.608	0.904
DMF	0.00	0.69	0.88	0.031	0.613	0.759	0.977
Acetonitrile	0.19	0.40	0.75	0.044	0.286	0.645	0.974
DMSO	0.00	0.76	1.00	0.072	0.647	0.830	1.000

The multi-linear regression analyses of $\bar{\upsilon}_{abs}$, $\bar{\upsilon}_{em}$ and $\Delta\bar{\upsilon}$ as a function of the Kamlet-Taft (equation 1) solvent scales were performed on compounds **5b** and **5f**, respectively. The estimated

coefficients y_0, a_α, b_β and c_{π^*} are tabulated in Table 5. In case of **5b**, the multi-linear analysis of the $\bar{\upsilon}_{abs}$ data according to Kamlet-Taft gives a poor fit as assessed by the low value of r (0.654) and the relatively large standard errors on a_α and b_β (except c_{π^*}). Further, the large negative c_{π^*} estimate compared to the a_α and b_β estimates clearly suggests that the small change of $\bar{\upsilon}_{abs}$ is mainly due to the change in polarizability of the environment of the chromophore. However, slightly better linear regression value (r = 0.702) is achieved in the fit of $\bar{\upsilon}_{em}$ as a function of Kamlet-Taft parameter. Also, the relatively large negative, estimate c_{π^*} with small standard error when compared to the other estimates with large standard errors indicate that solvent (di)polarity/polarizability is the main parameter responsible for the shift of $\bar{\upsilon}_{em}$.[52] But, the fit of Stoke shift $\Delta\bar{\upsilon}$ as a function of a_α, b_β and c_{π^*} parameters shows the relatively least linear relation (r = 0.593) and exhibits positive estimate a_α with small standard error relative to the rest of the estimates. Similarly, poor linear regression coefficients are obtained in compound **5f**.

Due to the poor multi-linear regression value of compounds **5b** and **5f** as a function of Kamlet-Taft solvent scale, another empirical solvent scale (Catalán) is utilized and it is expressed by the multi-linear equation (2).

$$y = y_0 + a_{SA}\,\mathrm{SA} + b_{SB}\,\mathrm{SB} + c_{SP}\,\mathrm{SP} + d_{SdP}\,\mathrm{SdP} \qquad (2)$$

Where SA, SB, SP and SdP represent acidity, basicity, solvent polarizability and solvent dipolarity, respectively and their values are given in Table 4; a_{SA}, b_{SB}, c_{SP} and d_{SdP} are the adjustable coefficients that reveal the sensitivity of the physicochemical property y in a given solvent to the various {SA, SB, SP and SdP} solvent parameters. The obtained data for compounds **5b** and **5f** as a function of Catalán parameters are tabulated in Table 5. Here, better linear regression coefficients are achieved in the fit of $\bar{\upsilon}_{abs}$, $\bar{\upsilon}_{em}$ and $\Delta\bar{\upsilon}$ as a function of {SA, SB, SP and SdP} compared to the data obtained by using equation (1). Also, the observed large,

negative, estimate c_{SP} with small standard error suggest that change in polarizability of the environment of the compound is the main cause for the observed shift in the $\bar{\upsilon}_{abs}$.

Table 5 Estimated coefficients (y_0, a_α, b_β, c_{π^*}, a_{SA}, b_{SB}, c_{SP} *and* d_{SdP}), their standard errors and correlation coefficients (r) for the multiple linear regression analyses of $\bar{\upsilon}_{abs}$, $\bar{\upsilon}_{em}$, $\Delta\bar{\upsilon}$ of **5b** and **5f** as a function of the Kamlet-Taft (equation 1) and Catalán (equation 2) solvent scales. For Kamlet-Taft and Catalán, 12 solvents were used in the analysis of $\bar{\upsilon}_{abs}$, $\bar{\upsilon}_{em}$, $\Delta\bar{\upsilon}$

Compound 5b						
Kamlet-Taft	y_0 **(10^3)**	a_α **(10^3)**	b_β **(10^3)**	c_{π^*} **(10^3)**		***r***
$\bar{\upsilon}_{abs}$	27.78±0.16	-0.16±0.21	0.26±0.30	-0.68±0.28		0.654
$\bar{\upsilon}_{em}$	23.75±0.58	-1.56±0.76	0.79±1.07	-1.97±1.00		0.702
$\Delta\bar{\upsilon}$	4.03±0.63	1.40±0.82	-0.52±1.15	1.28±1.08		0.593
Catalán	y_0 **(10^3)**	a_{SA} **(10^3)**	b_{SB} **(10^3)**	c_{SP} **(10^3)**	d_{SdP} **(10^3)**	***r***
$\bar{\upsilon}_{abs}$	29.52±0.49	-0.63±0.30	0.18±0.23	-2.82±0.73	-0.13±0.21	0.888
$\bar{\upsilon}_{em}$	23.10±2.79	-1.16±1.70	1.21±1.33	0.90±4.12	-2.25±1.18	0.712
$\Delta\bar{\upsilon}$	6.41±2.85	0.53±1.73	-1.03±1.36	-3.72±4.22	2.12±1.21	0.655
Compound 5f						
Kamlet-Taft	y_0 **(10^3)**	a_α **(10^3)**	b_β **(10^3)**	c_{π^*} **(10^3)**		***r***
$\bar{\upsilon}_{abs}$	27.83±0.14	-0.11±0.19	0.24±0.26	-0.74±0.25		0.732
$\bar{\upsilon}_{em}$	23.75±0.49	-0.80±0.64	1.86±0.90	-1.71±0.84		0.649
$\Delta\bar{\upsilon}$	4.07±0.48	0.69±0.63	-1.61±0.88	0.96±0.82		0.555
Catalán	y_0 **(10^3)**	a_{SA} **(10^3)**	b_{SB} **(10^3)**	c_{SP} **(10^3)**	d_{SdP} **(10^3)**	***r***
$\bar{\upsilon}_{abs}$	29.73±0.38	-0.57±0.23	-0.01±0.18	-3.06±0.56	-0.06±0.16	0.931
$\bar{\upsilon}_{em}$	23.43±1.95	-0.03±1.18	2.64±0.93	0.20±2.88	-1.93±0.83	0.781
$\Delta\bar{\upsilon}$	6.29±1.73	-0.54±1.05	-2.66±0.83	-3.26±2.57	1.87±0.74	0.784

Presently, luminescent mesogens are of great interest, as their self-assembling properties can be exploited to achieve linearly polarized electroluminescence for applications in emissive

displays.[53, 54] However, it is quite difficult to achieve both the properties in a single molecular architecture. As observed, the results of liquid crystal and photophysical studies on compounds **5a-j** clearly reveal that they exhibit wide hexagonal columnar phase ranging from ambient temperature to 90 ^{o}C and strong blue emission behavior in their liquid crystalline film state. The new design carrying electron deficient 1,2,3-triazole ring in combination with cyanopyridine unit augments good mesogenic and luminescent properties in them. Also, presence of two electron deficient units in their structure may possess improved charge carrier capability when compared to the compounds reported earlier. [29, 55]

Conclusion

In this paper we describe the design, synthesis and structural characterization of ten new 4-(3,4-bis(akyloxy)phenyl)-6-(4-((1-(4-cyano- or 4-nitro- benzyl)-1*H*-1,2,3-triazol-4-yl)methoxy)phenyl)-2-oxo-1,2-dihydropyridine-3-carbonitrile (**5a-j**) derivatives carrying terminal substituents, *viz.* polar groups (-CN or $–NO_2$) and variable alkoxy chain lengths. The ambient temperature columnar phase was successfully achieved in the new designs by introducing two highly electron deficient motifs, *viz.* cyanopyridone and 1,2,3-triazole moieties. Further, the increase in chain lengths of terminal alkoxy substituent enhances the clearing temperature and thermal range of the observed columnar phase. PXRD measurements combined with textural observations evidences the existence of columnar phase with hexagonal symmetry, which is due to the presence of hydrogen bonds and the participation of cyano functional group in dimerization. The crystal structure analysis of compound **3a** further confirms the dimer structure. The compounds **5a-j** exhibit an identical strong absorption band at ~ 370 nm and blue emission band at ~ 466 nm in chloroform. The observed bathochromic shift of ~ 10 nm in the emission band of compounds in their liquid crystalline phase is attributed to the lowering of

energy levels because of intimate overlap of molecular cores in the hexagonal columnar phase. Further, the compounds display good quantum yield of 0.60-0.62 with reference to quinine sulphate. Also, solvatochromic behavioral study reveals that the absorption bands are red shifted, while emission bands are independent with the increase of solvent polarity. Thus, mesogenic and photophysical studies reveal that new compounds are potential candidates for their applications in electronic devices.

† Electronic supplementary information (ESI) available: ORTEP diagram and crystal data of **3a**, PXRD data of **5b** and **5f**. Crystallographic data for the structure reported in this article has been deposited with the Cambridge Crystallographic Data Center with the deposition number 966496. Copy of the data can be obtained free of charge from the Director, CCDC, 12 Union Road, Cambridge CB2 1EZ, UK [Fax: +44-1223-336-033; E-mail: deposit@ccdc.cam.ac.uk or www.ccdc.cam.ac.uk].

Acknowledgment

The authors are grateful to the NITK, Surathkal, NMR research centre, and Solid State Structural Chemistry Unit, IISc, Bangalore for necessary facilities.

References

1. M. P. Aldred, A. J. Eastwood, S. M. Kelly, P. Vlachos, A. E. A. Contoret, S. R. Farrar, B. Mansoor, M. O'Neill and W. C. Tsoi, Light-emitting fluorene photoreactive liquid crystals for organic electroluminescence, *Chem. Mater.*, 2004, **16**, 4928–4936.
2. P. Vlachos, B. Mansoor, M. P. Aldred, M. O'Neill and S. M. Kelly, Charge-transport in crystalline organic semiconductors with liquid crystalline order, *Chem. Commun.*, 2005, 2921–2923.

3. A. Bacher, P. G. Bentley, P. A. Glarvey, M. Grell, K. S. Whitehead, D. D. C. Bradley and M. L. Turner, Conjugated reactive mesogens, *Synthetic Met.*, 2000, **111–112**, 413–415.
4. A. J. Eastwood, A. E. A. Contoret, S. R. Farrar, S. Fowler, S. M. Kelly, S. M. Khan, J. E. Nicholls and M. O'Neill, Synthesis and luminous properties of electroluminescent liquid crystals, *Synthetic Met.*, 2001, **121**, 1659–1660.
5. D. Haristoy and D. Tsiourvas, Novel ionic liquid-crystalline compounds bearing oxadiazole and pyridinium moieties as prospective materials for optoelectronic applications, *Chem. Mater.*, 2003, **15**, 2079–2083.
6. A. E. A. Contoret, S. R. Farrar, M. O'Neill, J. E. Nicholls, G. J. Richards, S. M. Kelly and A. W. Hall, The photopolymerization and cross-linking of electroluminescent liquid crystals containing methacrylate and diene photopolymerizable end groups for multilayer organic light-emitting diodes, *Chem. Mater.* 2002, **14**, 1477–1487.
7. S. Torgova and A. Strigazzi, Organic electroluminescent materials, *Mol. Cryst. Liq. Cryst.*, 2002, **375**, 61–72.
8. R. Giménez, M. Piñol and J. L. Serrano, Luminescent liquid crystals derived from 9,10-bis(phenylethynyl)anthracene, *Chem. Mater.*, 2004, **16**, 1377–1383.
9. M. Grell and D. D. C. Bradley, Polarized luminescence from oriented molecular materials, *Adv. Mater.,* 1999, **11**, 895–905.
10. R. Cai and E. T. Samulski, New thermotropic liquid crystals derived from thiophenes, *Liq. Cryst.*, 1991, **9**, 617–634.
11. R. Cristiano, E. Westphal, I. H. Bechtold, A. J. Bortoluzzi and H. Gallardo, Synthesis and optical/thermal properties of low molecular mass V-shaped materials based on 2,3-dicyanopyrazine, *Tetrahedron*, 2007, **63**, 2851–2858.

12. A. S. Matharu and D. Chambers-Asman, Structure–property investigation of 2- and 3-thienylacrylates bearing laterally fluorinated azobenzene moieties, *Liq. Cryst.*, 2007, **34**, 1317–1336.

13. H. Gallardo, C. Zucco and L. Da Silva, Synthesis and characterization of a new series of liquid crystal compounds derived from isoxazoles, *Mol. Cryst. Liq. Cryst.*, 2002, **373**, 181–190.

14. H. Gallardo, R. Magnago and A. J. Bortoluzzi, Synthesis, characterization and mesomorphic properties of Ag(I) and Pd(II) complexes containing the pyridyl and tetrazoyl rings: crystal structure of [C30H46N10AgClO4], *Liq. Cryst.*, 2001, **28**, 1343–1352.

15. A. Seed, Synthesis of self-organizing mesogenic materials containing a sulfur-based five-membered heterocyclic core, *Chem. Soc. Rev.*, 2007, **36**, 2046–2069.

16. M. Simard, D. Su and J. D. Wuest, Use of hydrogen bonds to control molecular aggregation. Self-assembly of three-dimensional networks with large chambers, *J. Am. Chem. Soc.*, 1991, **113**, 4696–4698.

17. M. Gallant, Phan Viet Minh Tan and J. D. Wuest, Hydrogen-bonded dimers. Direct study of the interconversion of pyridone dimers and hydroxypyridine monomers by low-temperature nuclear magnetic resonance spectroscopy, *J. Am. Chem. Soc.*, 1991, **113**, 721–723.

18. Y. Ducharme and J. D. Wuest, Use of hydrogen bonds to control molecular aggregation. Extensive, self-complementary arrays of donors and acceptors, *J. Org. Chem.*, 1988, **53**, 5787–5789.

19. R. Kleppinger, C. P. Lillya and C. Yang, Discotic liquid crystals through molecular self-assembly, *J. Am. Chem. Soc.*, 1997, **119**, 4097–4102.

20. H. Gallardo, F. Ely, A. J. Bortoluzzi and G. Conte, Applying click chemistry to synthesis of chiral [1,2,3]-triazole liquid crystals, *Liq. Cryst.*, 2005, **32**, 667–671.

21. R. Cristiano, D. M. P. de Oliveira Santos, G. Conte and H. Gallardo, 1,4-Diaryl and Schiff's base [1,2,3]-triazole derivative liquid crystalline compounds, *Liq. Cryst.*, 2006, **33**, 997–1003.

22. D. Srividhya, S. Manjunathan, S. Thirumaran, C. Saravanan and S. Senthil, Synthesis and characterization of [1,2,3]-triazole containing liquid crystals through click reaction, *J. Mol. Struct.*, 2009, **927**, 7–13.

23. M. -H. Ryu, J. -W. Choi and B. -K. Cho, Design, synthesis, and self-assembly behavior of *C3*-symmetry discotic molecules via click chemistry, *J. Mater. Chem.*, 2010, **20**, 1806–1810.

24. H. Gallardo, A. J. Bortoluzzi and D. M. P. De Oliveira Santos, Synthesis, crystalline structure and mesomorphic properties of new liquid crystalline 1,2,3-triazole derivatives, *Liq. Cryst.,* 2008, **35**, 719–725.

25. G. Conte, F. Ely and H. Gallardo, An investigation of the synthesis of chiral LCs based on the [1,2,3]-triazole ring, *Liq. Cryst.*, 2005, **32**, 1213–1222.

26. M. Dušek, V. Petříček, M. Wunschel, R. E. Dinnebier and S. van Smaalen, Refinement of modulated structures against X-ray powder diffraction data with JANA 2000, *J. Appl. Crystallogr.*, 2001, **34**, 398–404.

27. Bruker, APEX2, GIS, SADABS and SAINT Bruker AXS Inc., Madison, Wisconsin, USA, 2009.

28. G. M. Sheldrick, A short history of SHELX, Acta Crystallogr. Sect. A, 2007, **64**, 112–122.

29. T. N. Ahipa and A. V. Adhikari, Trihydrazone functionalized cyanopyridine discoids: synthesis, mesogenic and optical properties, *Tetrahedron Lett.*, 2014, **55**, 495–500.

30. V. V. Rostovtsev, L. G. Green, V. V. Fokin and K. B. Sharpless, A Stepwise Huisgen Cycloaddition Process: Copper (I)-Catalyzed Regioselective "Ligation" of Azides and Terminal Alkynes, *Angew. Chem. Int. Edit.*, 2002, **41**, 2596–2599.

31. M. Gil, M. Arévalo and Ó. López, Click Chemistry - What's in a Name? Triazole Synthesis and Beyond, *Synthesis*, 2007, 1589–1620.

32. C. W. Tornøe, C. Christensen and M. Meldal, Peptidotriazoles on Solid Phase: [1,2,3]-Triazoles by Regiospecific Copper(I)-Catalyzed 1,3-Dipolar Cycloadditions of Terminal Alkynes to Azides, *J. Org. Chem.*, 2002, **67**, 3057–3064.

33. S. Ulloora, R. Shabaraya and A. V. Adhikari, Facile synthesis of new imidazo[1,2-a]pyridines carrying 1,2,3-triazoles via click chemistry and their antiepileptic studies, *Bioorg. Med. Chem. Lett.*, 2013, **23**, 3368–3372.

34. I. H. Ibrahim, and W. Haase, On the Molecular Polarizability of Nematic Liquid Crystals. *Mol. Cryst. Liq. Cryst.*, 1981, **66**, 189–198.

35. G. A. Crosby and J. N. Demas, Measurement of photoluminescence quantum yields. Review, *J. Phys. Chem.*, 1971, **75**, 991–1024.

36. J. R. Lakowicz, Principles of Fluorescence Spectroscopy, 2nd ed.; Kulwer Academic: New York, 1999, 52–54.

37. J. R. Lakowicz, Principles of Fluorescence Spectroscopy, 2nd ed.; Kulwer Academic: New York, 1999, 187–194.

38. E. Lippert, *Z. Elektrochem*, 1957, **61**, 962–975.

39. K. N. Mataga, Y. Kaifu and M. Koizumi, *Bull. Chem. Soc. Jpn.*, 1956, **29**, 465–470.

40. N. K. Petrov, D. E. Markov, M. N. Gulakov, M. V. Alfimov and H. Staerk, Study of preferential solvation in binary mixtures by means of frequency-domain fluorescence spectroscopy, *J. Fluoresc.*, 2002, **12**, 19–24.

41. N. K. Petrov, A. Wiessner and H. Staerk, A simple kinetic model of preferential solvation in binary mixtures, *Chem. Phys. Lett.*, 2001, **349**, 517–520.

42. S. G. Schulman, R. W. Townsend and W. R. G. Baeyens, Proton-transfer kinetics of photoexcited 2-hydroxybiphenyl in aqueous methanol solutions. *Anal. Chim. Acta.*, 1995, **303**, 25–29.

43. S. Kim, D. W. Chang, S. Y. Park, H. Kawai and T. Nagamura, Excited state intramolecular proton transfer in a dendritic macromolecular system: poly(aryl ether) dendrimers with photoautomerizable quinolone core, *Macromolecules*, 2002, **35**, 2748–2753.

44. C. Carmona, M. Balón, M. Galán, P. Guardado and M. A. Munoz, Dynamic study of excited state hydrogen-bonded complexes of harmane in cyclohexane-toluene mixtures, *Photochem. Photobiol.*, 2002, **76**, 239–246.

45. T. Molotsky and D. Huppert, Solvation statics and dynamics of coumarin 153 in hexane-propionitrile solvent mixtures, *J. Phys. Chem. A.*, 2002, **106**, 8525–8530.

46. S. Fery-Forgues, J-P. Fayet and A. Lopez, Drastic changes in the fluorescence properties of NBD probes with the polarity of the medium: involvement of a TICT state, *J. Photochem. Photobiol. A: Chem*., 1993, **70**, 229–243.

47. S. Mazères, V. Schram. J-F. Tocanne and A. Lopez, 7-nitrobenz-2-oxa-1,3-diazole-4-yl-labeled phospholipids in lipid membranes: differences in fluorescence behavior, *Biophys. J.*, 1996, **71**, 327–335.

48. M. J. Kamlet and R.W. Taft, Solvatochromic comparison method. 1. β-Scale of solvent hydrogen-bond acceptor (HBA) basicities, *J. Am. Chem. Soc.*, 1976, **98**, 377–383.

49. R. W. Taft and M. J. Kamlet, Solvatochromic comparison method. 2. α-Scale of solvent hydrogenbond donor (HBD) acidities, *J. Am. Chem. Soc.*, 1976, **98**, 2886–2894.

50. M. J. Kamlet, J. L. M. Abboud and R. W. Taft, Solvatochromic comparison method. 6. π* Scale of solvent polarities, *J. Am. Chem. Soc.*, 1977, **99**, 6027–6038.

51. J. Catalán, Toward a Generalized Treatment of the Solvent Effect Based on Four Empirical Scales: Dipolarity (SdP, a New Scale), Polarizability (SP), Acidity (SA), and Basicity (SB) of the Medium, *J. Phys. Chem. B*, 2009, **113**, 5951–5960.

52. A. Filarowski, M. Kluba, K. Cieślik-Boczula, A. Koll, A. Kochel, L. Pandey, W. M. De Borggraeve, M. V. der Auweraer, J. Catalán and N. Boens, Generalized solvent scales as a tool for investigating solvent dependence of spectroscopic and kinetic parameters. Application to fluorescent BODIPY dyes, *Photochem. Photobiol. Sci.*, 2010, **9**, 996–1008.

53. R. Gimenez, M. Pinol and J. L. Serrano, Luminescent liquid crystals derived from 9,10-*bis*(phenylethynyl)anthracene, *Chem. Mater.*, 2004, **16**, 1377–1383.

54. H. Tokuhisa, M. Era and T. Tsutsui, Polarized electroluminescence from smectic mesophase, *Appl. Phys. Lett.*, 1998, **72**, 2639–2641.

55. T. N. Ahipa, Vijith Kumar, D. S. Shankara Rao, S. Krishna Prasad and A. V. Adhikari, New 4-(2-(4-alkoxyphenyl)-6-methoxypyridin-4-yl)benzonitriles: Synthesis, liquid crystalline behavior and photophyscial properties, CrystEngComm, 2014, **16**, 5573-5582.